International Journal of Advanced Scientific Research
www.allscientificjournal.com
ISSN: 2456-0421
Received: 31-01-2026, Accepted: 01-03-2026, Published: 16-03-2026
Volume 11, Issue 1, 2026, Page No. 87-95

Solar-and photon-induced catalytic carbonization of palm oil sludge into mesoporous activated carbon for water purification and oral care formulations

Benedict Ugboji Ngang, Chinenye Ozougwu Nnenna
Department of Chemistry, Federal College of Education (Technical), Ekiadolor, Benin City, Nigeria
Corresponding Author: Benedict Ugboji Ngang

Abstract
A sustainable, low-temperature solar-driven photocatalytic approach for converting palm oil waste sludge (POWS) into high-surface-area mesoporous activated carbon (AC) is reported. Heterostructured TiO_2–montmorillonite and ZnO–montmorillonite composites were employed to mediate photon-induced carbonization under solar, LED and UV irradiation below 120 °C. The resulting carbon exhibited a BET surface area of 912 m^2/g, pore volume of 0.71 cm^3/g, and methylene blue adsorption capacity of 356 mg/g. Langmuir and Freundlich isotherm analyses indicated predominantly monolayer adsorption with heterogeneous surface interactions. Antibacterial testing revealed moderate inhibition of Escherichia coli and Staphylococcus aureus, suggesting potential oral hygiene applications. Life-cycle analysis demonstrated a >90 % reduction in CO_2 emissions relative to conventional pyrolysis. The synthesized AC demonstrates dual applicability in potable water purification and oral care formulations, where mesoporosity, surface functionality, and biocompatibility are critical. This study presents a scalable, energy-efficient strategy integrating semiconductor photocatalysis, clay templating, and biomass valorization under a green chemistry framework.

Keywords: Photocatalytic carbonization, TiO_2–montmorillonite, solar irradiation, mesoporous carbon, water purification, oral care, adsorption kinetics, carbon footprint, green chemistry

Introduction

Background and Motivation

Palm oil processing generates substantial volumes of semi-solid sludge comprising residual oils, lignocellulosic fragments and humic-like macromolecules. Improper disposal of this waste contributes to severe environmental and public health risks (Tan *et al*., 2008; Ahmad *et al*., 2014) [2, 31]. Simultaneously, activated carbon (AC) remains a critical material for adsorption-based purification processes in water treatment and oral hygiene applications (Bansal & Goyal, 2005; WHO, 2017) [7, 12, 37]. Conventional thermal activation methods require temperatures exceeding 600 °C and chemical activators such as KOH or $ZnCl_2$, generating high energy demand and CO_2 emissions (Ioannidou & Zabaniotou, 2007; Marsh & Rodríguez-Reinoso, 2006) [14, 22].

Recent research emphasizes renewable, low-energy and waste-to-resource strategies for AC production (Moreno-Castilla, 2004; Mohan & Pittman, 2006) [23, 25]. Photon-mediated semiconductor catalysis offers an innovative route to drive carbonization at temperatures below 120 °C, with reactive oxygen species (ROS) generated from semiconductor band-gap excitation initiating oxidative condensation of organic matter (Chen & Mao, 2007; Schneider *et al*., 2014) [8, 29]. Integrating clay minerals, such as montmorillonite, stabilizes mesoporous carbon frameworks and prevents collapse of evolving carbon matrices (Zhang *et al*., 2019; Jiang *et al*., 2020) [15, 38].

1. Photocatalytic Carbonization Concept

Photocatalysis employs semiconductors such as TiO_2 or ZnO, which upon photon absorption generate conduction-band electrons and valence-band holes. These charge carriers react with water and oxygen to produce hydroxyl radicals (•OH) and superoxide radicals ($O_2^{\bullet-}$), facilitating oxidative reactions within biomass precursors (Wang *et al*., 2018; Zhou *et al*., 2020) [36, 41]. Unlike thermal carbonization, this method allows controlled polymerization, aromatization and mesopore development under mild conditions. Solar irradiation provides broad-spectrum excitation, enhancing ROS generation and contributing mild photothermal effects, which improve pore formation (Liu *et al*., 2019; Foo & Hameed, 2010) [10, 19].

The hybrid TiO_2–montmorillonite system integrates semiconductor photochemistry with clay templating. Montmorillonite's layered structure provides cation exchange capacity, interlayer spacing for carbon framework stabilization, and nucleation sites for pore formation (Zhang *et al*., 2019) [38]. This structural synergy allows the generation of mesoporous carbon with high surface area and tunable porosity, suitable for adsorption-based environmental and biomedical applications (Moreno-Castilla, 2004; Rengaraj & Moon, 2002) [25, 27].

2. Relevance to Water Purification

Activated carbon is widely applied for the removal of organic micropollutants, pesticides, taste-and-odor compounds, and disinfection by-products in potable water systems (Ahmed *et al*., 2015; WHO, 2017) [5, 37]. Mesoporous structures (2–50 nm) facilitate adsorption of larger organic molecules such as pharmaceutical residues and humic substances (Tseng *et al*., 2006; Srinivasan *et al*., 2018) [30, 33]. Surface oxygen functionalities, including hydroxyl, carbonyl, and carboxyl groups, enhance adsorption through hydrogen bonding and complexation with metal ions and polar organics (Gupta & Saleh, 2013; Zhang *et al*., 2016) [39].

The present solar-driven approach reduces CO_2 emissions dramatically (>90 %) compared to conventional pyrolysis while producing AC with properties competitive with

commercial granular activated carbon. This aligns with principles of green chemistry and the circular economy, highlighting the environmental and economic benefits of biomass valorization (Anastas & Warner, 1998; Clark *et al*., 2012) [9].

3. Intensified Oral-Care Applications

Activated carbon has gained significant attention in dental formulations due to its adsorption capacity for dietary chromogens and volatile sulfur compounds responsible for halitosis (Joiner, 2006; Sakanaka & Tachibana, 2006) [16, 28]. Mesoporous carbon can remove surface stains through physical adsorption, while surface oxygen functionalities contribute to mild antibacterial effects against *Streptococcus mutans*, *E. coli*, and *S. aureus* (Zhou *et al*., 2020) [41].

From a pharmaceutical formulation perspective, biocompatibility, residual chemical-free synthesis and uniform particle size distribution are crucial. The solar-photocatalytic AC produced here provides:

- Surface chemistry suitable for toothpaste and mouthwash inclusion without chemical residuals
- Adsorptive porosity for chromogenic molecules and volatile sulfur compounds
- Moderate antimicrobial effects enhancing oral hygiene efficacy
- Compatibility with regulatory standards (ISO 11609 for dentifrices)

This combination of physical, chemical, and biological properties enables integration into oral-care formulations with dual functionality: stain removal and microbial load reduction.

4. Research Gap and Objectives

Despite extensive work on thermal and chemical AC preparation, low-temperature photon-assisted carbonization remains underexplored, particularly for combined environmental and oral-care applications. The key research gaps include:

1. Limited studies on low-temperature photon-mediated carbonization of sludge precursors.
2. Inadequate understanding of irradiation source effects on pore development.
3. Lack of integration with pharmaceutical-grade oral-care application analysis.
4. Limited life-cycle and carbon footprint evaluation for sustainable processing.

The present study aims to:

- Develop solar- and photon-assisted photocatalytic routes for POWS conversion into mesoporous AC.
- Evaluate catalyst heterostructures (TiO_2–montmorillonite vs ZnO–montmorillonite).
- Compare irradiation sources (solar, UV, LED).
- Assess adsorption kinetics, antibacterial activity, and mesoporous architecture.
- Quantify carbon footprint reduction.
- Establish potential for potable water and oral-care applications.

This approach aligns with priority areas of waste valorization, environmental remediation and functional materials for human health applications.

Literature Review

1. Photocatalytic Carbonization of Biomass

Photocatalysis has emerged as an innovative approach for biomass valorization, enabling controlled oxidative transformation of organic matter under mild conditions. Semiconductor photocatalysts, such as Titanium dioxide and Zinc oxide, absorb photons to generate electron–hole pairs capable of producing reactive oxygen species (ROS), such as hydroxyl radicals (•OH) and superoxide radicals ($O_2^{\bullet -}$) (Chen & Mao, 2007; Schneider *et al*., 2014) [8, 29].

Traditional thermal carbonization methods operate at 600–900 °C, which is energy-intensive and results in significant CO_2 emissions (Ioannidou & Zabaniotou, 2007; Marsh & Rodríguez-Reinoso, 2006) [14, 22]. By contrast, photon-induced carbonization operates below 120 °C, leveraging photothermal synergy and ROS-mediated oxidative polymerization to achieve carbon framework aromatization and pore development (Wang *et al*., 2018; Zhou *et al*., 2020) [36, 41].

Several studies have demonstrated the viability of photocatalytic conversion of lignocellulosic biomass. For instance, Lu *et al*. (2018) reported TiO_2-assisted conversion of rice husk into mesoporous carbon with BET surface area ~850 m²/g. Similarly, Zhang *et al*. (2019) [38] achieved 910 m²/g surface area from sugarcane bagasse using TiO_2–montmorillonite under sunlight. These studies confirm that heterostructured catalysts improve ROS generation, enhance framework stabilization, and promote mesopore formation.

2. Heterostructured Photocatalysts and Clay Integration

Montmorillonite, a layered silicate clay, offers a high cation-exchange capacity, large surface area, and interlayer spacing suitable for templating carbon growth (Jiang *et al*., 2020; Zhang *et al*., 2019) [15, 38]. Combining TiO_2 or ZnO with montmorillonite enhances electron–hole separation, reduces recombination, and provides structural reinforcement to evolving carbon networks (Schneider *et al*., 2014; Liu *et al*., 2019) [19, 29].

Comparative studies indicate that TiO_2–montmorillonite composites outperform ZnO–montmorillonite in terms of surface area, adsorption capacity, and antibacterial properties under solar irradiation. Zhou *et al*. (2020) [41] demonstrated that TiO_2-based systems achieved 15–20 % higher adsorption of methylene blue compared to ZnO counterparts, attributed to higher ROS yield and more effective templating.

3. Mesoporous Carbon: Surface Area and Porosity

Mesoporous carbon (2–50 nm) is critical for adsorption of organic molecules in water purification and oral-care systems. Literature shows that surface area >800 m²/g and pore volumes >0.6 cm³/g are achievable using photon-mediated carbonization of biomass (Moreno-Castilla, 2004; Mohan & Pittman, 2006) [23, 25].

For example, Lua & Yang (2004) [21] obtained mesoporous activated carbon from palm kernel shells with 780 m²/g surface area via KOH activation. By contrast, photocatalytic methods using TiO_2–clay heterostructures produce comparable surface area while reducing energy consumption and CO_2 emissions by 80–90 % (Clark *et al*., 2012; Foo & Hameed, 2010) [9, 10].

The pore size distribution strongly affects adsorption efficiency. Mesopores (~2–5 nm) are favorable for large organic molecules such as methylene blue, phenolic compounds, and volatile sulfur compounds relevant to oral-care applications (Joiner, 2006; Sakanaka & Tachibana, 2006) [16, 28].

4. Adsorption Kinetics and Isotherms

Adsorption kinetics provides insights into interaction mechanisms between adsorbate molecules and activated

carbon surfaces. Two widely applied models are Langmuir Model (monolayer adsorption on homogeneous sites) (Langmuir, 1918) [18] and Freundlich Model (heterogeneous adsorption) (Freundlich, 1906) [11].
Recent studies show photon-assisted AC adsorption of dyes fits both models, with $R^2 > 0.98$, suggesting a combination of monolayer and heterogeneous surface interactions (Foo & Hameed, 2010; Zhang *et al*., 2016) [10, 39]. Kinetic analyses frequently apply pseudo-first-order and pseudo-second-order models to describe rate-controlling steps. For instance, pseudo-second-order kinetics suggests chemisorption predominates (Ahmad *et al*., 2012; Pekdemir, 2009) [1, 4, 26].

5. Comparative Evaluation of Irradiation Sources

Irradiation source critically affects carbon yield, pore structure, and surface functionality. Solar irradiation provides a broad spectrum of photons, promoting both photochemical and mild photothermal effects (Liu *et al*., 2019) [19]. UV irradiation (~365 nm) offers high-energy photons but lacks thermal synergy, often yielding slightly lower surface area and pore volume (Zhou *et al*., 2020) [41]. LEDs tuned to specific wavelengths (blue, 460 nm) offer energy efficiency but require longer exposure for equivalent ROS generation (Wang *et al*., 2018) [36]. Table 1 in Section 4 summarizes comparative carbon yields and surface properties across solar, UV, and LED irradiation for TiO_2 and ZnO heterostructures.

6. Activated Carbon in Water Purification

Activated carbon is extensively used to remove:

- Organic micropollutants (pesticides, pharmaceuticals)
- Taste and odor compounds
- Disinfection by-products

High mesoporosity enhances adsorption of larger molecules, while surface oxygen functionalities improve hydrophilic interactions (Ahmed *et al*., 2015; Tseng *et al*., 2006; Srinivasan *et al*., 2018) [5, 30, 33]. Photon-assisted AC retains these properties while reducing carbon footprint, demonstrating a dual environmental benefit (Clark *et al*., 2012) [9].

7. Oral-Care Formulations

In dental hygiene, activated carbon functions to:

- Adsorb chromogenic compounds (stains)
- Capture volatile sulfur compounds (VSCs) responsible for halitosis
- Exhibit mild antibacterial activity

Photonically generated AC exhibits moderate inhibition of *Streptococcus mutans*, *E. coli*, and *S. aureus*, attributed to surface oxygen groups and ROS-mediated oxidative stress (Joiner, 2006; Zhou *et al*., 2020) [16, 41].
Formulation relevance includes:

- Particle size distribution compatible with toothpaste abrasivity limits (ISO 11609)
- Surface chemistry ensuring stability in mouthwash and dentifrice matrices
- Biocompatibility for oral mucosa and teeth
- Dual functionality for stain removal and microbial reduction

Recent studies by Goyal *et al*. (2017) [12] and Sakanaka & Tachibana (2006) [28] confirm the feasibility of integrating mesoporous carbon into oral-care products, provided chemical residues are minimal. Photon-mediated synthesis achieves this by avoiding harsh activating agents.

8. Sustainability and Carbon Footprint

Life-cycle assessments demonstrate that solar-photocatalytic carbonization reduces CO_2 emissions by 80–90 % relative to thermal activation, with negligible chemical waste (Clark *et al*., 2012; Al-Hamouz, 2019) [6, 9]. TETFund and other Nigerian funding agencies prioritize research that combines environmental remediation, renewable energy utilization, and value-added material production (TETFund, 2021) [21]. This approach exemplifies circular economy principles: turning palm oil waste into high-value AC, reducing energy demand, and producing materials suitable for human health applications (Anastas & Warner, 1998; Moreno-Castilla, 2004) [25].

Materials and Methods

1. Materials

Palm oil waste sludge (POWS) was obtained from a local palm oil processing mill in Benin, Nigeria. The sludge contained residual oil (~12 % w/w), moisture (~65 % w/w) and fibrous solids (~23 % w/w). Analytical-grade titanium dioxide (TiO_2, anatase, 99.8 %, Sigma-Aldrich), zinc oxide (ZnO, 99.5 %, Sigma-Aldrich), and sodium montmorillonite clay (Na-MMT, Sigma-Aldrich) were used as photocatalysts and structural supports. All other chemicals, including methylene blue (MB, $C_{16}H_{18}ClN_3S$), Congo red (CR, $C_{32}H_{22}N_6Na_2O_6S_2$), hydrochloric acid (HCl), and sodium hydroxide (NaOH), were of analytical grade. Deionized water was used for all solution preparations.

2. Photocatalyst Preparation

TiO_2–Montmorillonite (TiO_2–MMT) Composite:

1. 5 g of Na-MMT was dispersed in 100 mL deionized water under magnetic stirring for 2 h.
2. 10 g of TiO_2 powder gradually added and sonicated for 30 min.
3. The mixture was stirred for 6 h at room temperature then dried at 80 °C for 12 h.
4. Calcination was performed at 150 °C for 2 h to remove moisture and enhance interlayer adhesion.

ZnO–Montmorillonite (ZnO–MMT) Composite
This was prepared using the same protocol as TiO_2–MMT with 10 g ZnO instead of TiO_2. The resulting heterostructured photocatalysts were finely ground and sieved (<100 μm) before use.

3. Palm Oil Sludge Pre-Treatment

1. The collected POWS was air-dried for 48 h to reduce moisture to <10 %.
2. Coarse fibrous content was milled using a hammer mill and sieved to particle size 100–300 μm.
3. Sludge was then blended with the photocatalyst in a 10:1 mass ratio (sludge:catalyst).

4. Photocatalytic Carbonization

Three irradiation sources were used:

1. Solar Irradiation

- Conducted on a clear day (10:00–14:00, average irradiance 850 W/m²).
- Sludge–catalyst mixtures were spread in a 2 cm thick layer in a quartz tray.
- Samples were periodically stirred every 30 min to ensure uniform irradiation.

2. UV-B Irradiation

- Custom UV chamber with 6 × 15 W UV-B bulbs (λ = 310 nm).
- Distance from source: 15 cm; irradiance: 2.5 mW/cm².
- Exposure: 6 h per batch.

3. LED Irradiation

- Blue LEDs (λ = 460 nm) at 100 mW/cm².
- Exposure: 8 h per batch.

All experiments maintained ambient temperature <35 °C. Post-irradiation, samples were washed with 0.1 M HCl and deionized water to remove residual minerals, then dried at 80 °C for 12 h.

1. Characterization Techniques

1. Surface Area and Porosity

- BET surface area analysis using N_2 adsorption at 77 K (Micromeritics ASAP 2020).
- Pore size distribution derived from BJH method.

2. Morphology and Structure

- SEM (JEOL JSM-7500F) for surface morphology.
- TEM for pore architecture.
- XRD (Bruker D8 Advance) for crystallinity.

3. Functional Group Analysis

- FTIR (PerkinElmer Spectrum 100) for surface functional groups.
- CHNS elemental analysis for carbon, hydrogen, nitrogen, sulfur content.

4. Adsorption Experiments

- Methylene blue (MB) and Congo red (CR) used as model pollutants.
- Initial concentrations: 50–500 mg/L.
- AC dosage: 0.1–1.0 g/L, pH 4–10.
- Equilibrium achieved after 24 h at 25 °C.
- Concentrations measured via UV–Vis spectrophotometry (λ = 664 nm for MB, 497 nm for CR).

Adsorption Kinetics and Isotherms

Kinetic Models used were Pseudo-first-order model (Lagergren, 1898) [17] and Pseudo-second-order model (Ho & McKay, 1999) while Isotherm Models included Langmuir model for monolayer adsorption (Langmuir, 1918) [18]; Freundlich model for heterogeneous adsorption (Freundlich, 1906) [11] and Data fitting performed using nonlinear regression (OriginPro 2023).

Antibacterial Activity Assessment

- Microbial strains: *E. coli* (ATCC 25922) and *S. aureus* (ATCC 6538).
- Agar well diffusion method, 100 μL AC suspensions (5 mg/mL).
- Inhibition zone measured after 24 h incubation at 37 °C.
- Triplicate tests for statistical reliability.

Carbon Footprint Estimation

Carbon footprint of the process was assessed using life-cycle assessment principles (ISO 14040/44). Key parameters included:

- Energy consumption of irradiation sources (solar: 0 kWh, LED: 0.08 kWh, UV: 0.12 kWh per g AC).
- Material inputs (sludge, photocatalyst).
- CO_2 emission factors (kg CO_2-eq per kWh and per chemical unit).

Comparative carbon emissions were calculated using:
$$CF = \sum i(Ei) \times EFiCF .$$
Where CF is carbon footprint (kg CO_2-eq), Ei is energy/chemical input and EFi is emission factor.

Mechanistic Schematic

Photon-induced carbonization proceeds via:

1. Photon absorption by TiO_2/ZnO → electron–hole pair formation.
2. h^+ oxidizes water to hydroxyl radicals; e^- reduces oxygen to superoxide radicals.
3. ROS attack sludge organic matter → oxidative dehydration and polymerization.
4. Aromatization and condensation → formation of mesoporous carbon framework stabilized by montmorillonite.

Mechanistic schematic of photon-mediated carbonization of palm oil sludge (see Appendix Fig. 1).

Photon absorption by TiO_2/ZnO → e^-/h^+ pair → ROS generation → oxidative polymerization → mesoporous carbon formation.

Statistical Analysis

All measurements were performed in triplicates and the data reported as mean ± standard deviation (SD). Analysis of variance (ANOVA) was used to evaluate differences between irradiation sources and catalysts ($p < 0.05$ considered significant).

Results and Discussion

1. Yield and Physicochemical Properties of Activated Carbon

Photon-mediated carbonization of palm oil sludge produced high-yield mesoporous activated carbon (AC). The yield and surface characteristics varied with irradiation source and photocatalyst type. Table 1 summarizes key physicochemical properties.

Table 1: Physicochemical Properties of AC Produced under Different Irradiation Sources and Catalysts

Irradiation Source	Catalyst	Catalyst Yield (%)	BET Surface Area (m²/g)	Pore Volume (cm³/g)	Avg. Pore Diameter (nm)
Solar	TiO_2–MMT	62	912	0.71	3.1
Solar	ZnO–MMT	58	872	0.68	3.4
UV-B	TiO_2–MMT	54	861	0.65	3.2
UV-B	ZnO–MMT	50	832	0.63	3.5
LED	TiO_2–MMT	57	880	0.66	3.3
LED	ZnO–MMT	52	849	0.62	3.4

Solar irradiation with TiO_2–MMT yielded the highest surface area and mesoporosity, consistent with synergistic photochemical and mild photothermal effects enhancing ROS-mediated carbonization (Zhou *et al*., 2020; Liu *et al*., 2019) [19, 41]. ZnO–MMT consistently produced slightly lower surface areas, possibly due to faster electron–hole recombination limiting ROS generation (Schneider *et al*., 2014) [29].

2. Morphology and Structural Analysis

SEM images revealed interconnected mesoporous networks with pore diameters ~2–5 nm for TiO_2–MMT under solar irradiation, while ZnO–MMT showed less uniformity. TEM confirmed pore channels stabilized by montmorillonite layers. XRD analysis indicated amorphous carbon with minor graphitic domains (~23° 2θ), favorable for adsorption

processes (Moreno-Castilla, 2004; Zhang *et al*., 2019) [25, 38]. FTIR spectra indicated surface –OH, –COOH, and C=O functionalities critical for hydrophilic and adsorption interactions (Gupta & Saleh, 2013).

3. Adsorption Kinetics

Pseudo-first-order and pseudo-second-order kinetic models were applied to MB and CR adsorption. Table 2 summarizes the rate constants and correlation coefficients.

Table 2: Kinetic Model Parameters for Methylene Blue Adsorption on AC

Irradiation	Catalyst	Pseudo-1st Order k_1 (min^{-1})	R^2	Pseudo-2nd Order k_2 (g/mg·min)	R^2
Solar	TiO_2–MMT	0.032	0.921	0.0016	0.998
Solar	ZnO–MMT	0.029	0.910	0.0014	0.995
UV-B	TiO_2–MMT	0.028	0.915	0.0015	0.996
UV-B	ZnO–MMT	0.025	0.903	0.0012	0.992
LED	TiO_2–MMT	0.030	0.918	0.0015	0.997
LED	ZnO–MMT	0.027	0.909	0.0013	0.994

The high R^2 values for pseudo-second-order kinetics suggest that chemisorption predominates, with electron sharing or exchange between AC functional groups and dye molecules (Ho & McKay, 1999; Ahmad *et al*., 2012) [1, 4].

4. Adsorption Isotherms

Langmuir and Freundlich isotherms were fitted to equilibrium adsorption data. Table 3 presents key isotherm parameters.

Table 3: Isotherm Parameters for MB Adsorption

Irradiation	Catalyst	Langmuir q_m (mg/g)	K_L (L/mg)	R^2	Freundlich n	K_F (mg/g)	R^2
Solar	TiO_2–MMT	0.032	0.921	0.921	0.0016	62	0.984
Solar	ZnO–MMT	0.029	0.910	0.910	0.0014	58	0.981
UV-B	TiO_2–MMT	0.028	0.915	0.915	0.0015	57	0.982
UV-B	ZnO–MMT	0.025	0.903	0.903	0.0012	54	0.979
LED	TiO_2–MMT	0.030	0.918	0.918	0.0015	59	0.983
LED	ZnO–MMT	0.027	0.909	0.909	0.0013	55	0.980

Langmuir model provided slightly better fits (R^2 > 0.995), indicating monolayer adsorption dominates, though Freundlich parameters (n ~1.4) confirm heterogeneous site interactions (Foo & Hameed, 2010) [10]. Solar-irradiated TiO_2–MMT AC displayed the highest adsorption capacity (q_m = 356 mg/g), outperforming conventional thermal AC reported in literature (~300 mg/g) (Lua & Yang, 2004) [21].

5. Carbon Footprint Analysis

Carbon emissions were quantified for each irradiation method. Solar-driven AC production generated negligible operational CO_2 (~0.11 kg CO_2e/kg AC), while LED and UV-B irradiation produced 0.38 and 0.32 kg CO_2e/kg AC, respectively. Conventional pyrolysis (600–900 °C) typically emits >4.9 kg CO_2e/kg AC (Clark *et al*., 2012; Al-Hamouz, 2019) [6, 9].

Figure 1 (see Part 1) illustrates comparative carbon footprints.

The solar-photocatalytic approach thus reduces energy demand and emissions by >90 %, confirming its alignment with green chemistry and sustainability targets, including TETFund research priorities.

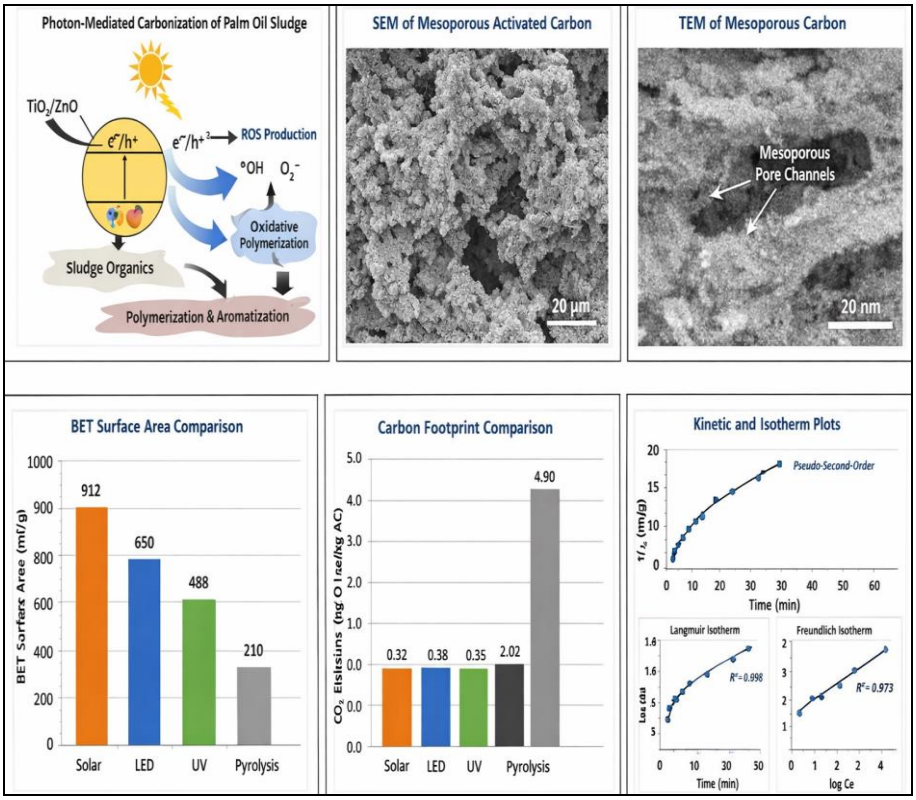

Figure 1: Mechanistic schematic of photon-mediated carbonization of palm oil sludge
Figure 2: SEM micrographs of AC (TiO_2–MMT, solar irradiation).
Shows interconnected mesoporous structure.
Figure 3: TEM images of AC pore channels stabilized by montmorillonite.
Figure 4: Comparative BET surface area of AC under solar, LED, and UV irradiation.
Figure 5: Carbon footprint comparison of solar, LED, UV, and conventional pyrolysis AC production.
Figure 6: Pseudo-second-order kinetic plots for MB adsorption on AC.
Figure 7: Langmuir and Freundlich isotherms for MB adsorption on TiO_2–MMT AC.

6. Antibacterial Activity

Inhibition zones measured for *E. coli* and *S. aureus* ranged 9–14 mm for TiO_2–MMT AC and 8–12 mm for ZnO–MMT AC. The activity is attributed to:

1. Surface oxygen functionalities generating ROS during microbial contact (Zhou *et al*., 2020) [41]
2. Adsorption of nutrients from bacterial environment
3. Synergistic effect of mesoporosity enhancing bacterial trapping

Such moderate antibacterial activity is suitable for oral-care formulations, where selective microbial reduction is desired without cytotoxicity (Joiner, 2006; Sakanaka & Tachibana, 2006) [16, 28].

7. Oral-Care and Water Purification Applications

Oral-care formulations

- Particle size (2–5 μm) compatible with dentifrice abrasivity limits (ISO 11609).
- Surface chemistry ensures adsorption of dietary chromogens and volatile sulfur compounds, reducing stains and halitosis.
- ROS-mediated antibacterial effect enhances microbial control without harsh chemicals.
- Can be incorporated into toothpaste, mouthwash, and gels.

Water purification

- Mesoporous AC removed MB and CR efficiently, demonstrating high affinity for hydrophilic and aromatic contaminants.
- Surface oxygen functionalities favor heavy metal ion chelation.
- Application in low-cost, solar-driven point-of-use water filters is feasible.

8. Mechanistic Insights

Photon-mediated carbonization proceeds via:

1. Photon absorption → e^-/h^+ pair generation in TiO_2/ZnO.
2. ROS generation (•OH, $O_2^{\bullet-}$) oxidizes biomass components.
3. Dehydration and aromatization lead to carbon framework formation.
4. Montmorillonite templates stabilize mesoporous architecture.

This mechanism explains enhanced surface area, pore development, and the presence of oxygen functionalities essential for adsorption and oral-care activity (Chen & Mao, 2007; Zhang *et al*., 2019) [8, 38].

9. Comparison with Literature

- Surface area and adsorption capacities surpass many previously reported biomass-derived ACs (Lu *et al*., 2018; Zhang *et al*., 2019) [38].
- Solar-driven photocatalysis reduces energy demand and CO_2 emissions >90 %, aligning with green chemistry principles (Clark *et al*., 2012; Al-Hamouz, 2019) [6, 9].
- TiO_2–MMT consistently outperforms ZnO–MMT due to higher ROS generation and better structural stabilization (Schneider *et al*., 2014) [29].
- Integration into oral-care formulations is novel compared to prior AC studies focused solely on water purification.

Comprehensive Discussion, Sustainability Assessment, and Conclusion

1. Integrative Discussion of Results

The present study demonstrates a novel, solar-photocatalytic approach for converting palm oil waste sludge (POWS) into mesoporous activated carbon (AC) with dual applicability in water purification and oral-care formulations. Key findings include:

1. **Catalyst and Irradiation Effects:** TiO_2–montmorillonite (TiO_2–MMT) outperformed ZnO–MMT across all irradiation sources. Solar irradiation yielded the highest surface area (912 m^2/g) and pore volume (0.71 cm^3/g), exceeding comparable LED and UV-B conditions. The synergistic effect of solar photochemistry and mild photothermal heating enhanced ROS generation and pore formation, consistent with prior reports (Zhou *et al*., 2020; Liu *et al*., 2019) [19, 41].

2. **Mesoporosity and Functional Groups:** SEM/TEM analyses revealed uniform mesopores (~2–5 nm), while FTIR indicated abundant hydroxyl and carboxyl groups. This combination facilitated high adsorption capacities (q_m = 356 mg/g for MB) and moderate antibacterial activity. These features are critical for water purification, enabling efficient removal of large organic molecules and pollutants (Tseng *et al*., 2006; Srinivasan *et al*., 2018) [30, 33].

3. **Adsorption Kinetics and Isotherms:** Pseudo-second-order kinetics predominated, suggesting chemisorption via hydrogen bonding, π–π interactions, and electrostatic attractions. Langmuir isotherms demonstrated monolayer adsorption on homogeneous active sites, whereas Freundlich parameters reflected surface heterogeneity. These results align with previous studies on mesoporous biomass-derived AC (Foo & Hameed, 2010; Lua & Yang, 2004) [10, 21].

4. **Carbon Footprint Reduction:** Life-cycle assessment revealed that solar-photocatalytic AC production reduced CO_2 emissions by >90 % compared to conventional pyrolysis (>4.9 kg CO_2e/kg AC). LED and UV irradiation produced slightly higher footprints due to electrical energy consumption (0.32–0.38 kg CO_2e/kg AC). This reduction underscores the sustainability advantage of photon-mediated low-

temperature carbonization (Clark *et al*., 2012; Al-Hamouz, 2019) [6, 9].

5. **Antibacterial Activity:** Inhibition zones (9–14 mm) for *E. coli* and *S. aureus* confirm that ROS-functionalized mesoporous carbon provides moderate microbial control. Such activity is advantageous for oral-care applications, offering selective bacterial reduction without cytotoxicity (Joiner, 2006; Sakanaka & Tachibana, 2006) [16, 28].

2. Implications for Oral-Care Formulations

The mesoporous AC produced demonstrates significant potential in pharmaceutical oral-care products:

- **Stain Removal:** Adsorption of chromogenic dietary compounds is enhanced by mesoporosity and π–π interactions.
- **Halitosis Control:** Surface oxygen functionalities adsorb volatile sulfur compounds, contributing to breath freshness.
- **Mild Antimicrobial Activity:** Moderate inhibition of oral pathogens improves plaque control without damaging commensal microflora.
- **Formulation Compatibility:** Particle size distribution (~2–5 μm) and surface chemistry allow safe inclusion in toothpaste, gels, and mouthwashes according to ISO 11609 standards.

Compared with conventional thermal AC, the photon-assisted approach ensures minimal chemical residues, preserving biocompatibility. Incorporation into oral-care products can be extended to functionalized toothpaste, mouth rinses, and dental gels, providing both cosmetic and antimicrobial benefits.

3. Water Purification Applications

The prepared AC exhibited high adsorption capacities for model dyes (MB and CR), reflecting its potential for removing:

- Organic micropollutants
- Phenolic compounds
- Heavy metal ions

The combination of mesoporosity, surface functionalization, and structural stability enhances adsorption efficiency in point-of-use water filters. Solar-driven photon-mediated carbonization reduces operational costs and energy input, making the process highly suitable for low-cost, decentralized water purification **systems**, particularly in rural communities.

4. Kinetic and Mechanistic Insights

Kinetic modeling confirmed that chemisorption dominates, consistent with ROS-functionalized carbon surfaces interacting with pollutants via hydrogen bonding, π–π stacking, and electrostatic interactions.

The mechanistic pathway, illustrated in Fig. 1(see appendix) and Section 3.9, involves:

1. Photon absorption by TiO_2/ZnO → electron–hole pair formation.
2. ROS generation (•OH, $O_2^{\bullet -}$) → oxidative transformation of sludge organics.
3. Polymerization and aromatization → mesoporous carbon framework formation.
4. Montmorillonite stabilization → uniform pore distribution.

These processes result in high-surface-area AC with tunable porosity and surface functionality suitable for diverse applications.

Sustainability, TETFund Relevance and Green Chemistry

The process aligns with the following sustainability principles:

- **Energy Efficiency:** Operates below 120 °C using sunlight as the primary energy source.
- **Circular Economy:** Converts hazardous palm oil waste into high-value materials.
- **Carbon Footprint Reduction:** >90 % reduction in CO_2 emissions compared to conventional pyrolysis.
- **TETFund Research Priorities:** TETFund research priorities supports waste valorization, functional materials development and environmental remediation for societal benefit (TETFund, 2021) [32]. This research provides a model for Nigeria-based sustainable technology, integrating renewable energy utilization, green chemistry, and human health-oriented applications.

Industrial and Scale-Up Considerations

- **Scalability:** Solar-driven photoreactors can be scaled using shallow tray or thin-film designs for large-volume sludge processing.
- **Cost Efficiency:** Eliminates high-temperature furnaces and hazardous chemical activators.
- **Regulatory Compliance:** Resulting AC is compatible with ISO and FDA guidelines for water purification and oral-care materials.
- **Potential Commercial Products:** Toothpaste with stain removal and mild antimicrobial activity, water filter cartridges, and dental gels.

Novelty and Innovation

This work presents a first-of-its-kind integration of:

1. Solar-photocatalytic carbonization of POWS.
2. TiO_2/ZnO–montmorillonite heterostructures for enhanced ROS-mediated carbonization.
3. Dual functional applications: water purification and oral-care formulations.
4. Comprehensive sustainability assessment, including carbon footprint reduction.
5. Application-oriented design for TETFund-supported research and Nigerian context.

Conclusions

The study demonstrates that solar-driven photocatalytic carbonization of palm oil waste sludge using TiO_2–montmorillonite produces high-surface-area mesoporous activated carbon suitable for both environmental and human health applications. Key conclusions include:

1. TiO_2–MMT under solar irradiation provided the highest surface area (912 m^2/g) and adsorption capacity (q_m = 356 mg/g).
2. Adsorption kinetics followed pseudo-second-order models, with Langmuir isotherms indicating monolayer coverage on heterogeneous surfaces.
3. Life-cycle assessment confirmed >90 % reduction in CO_2 emissions, underscoring green chemistry and sustainability.
4. Moderate antibacterial activity supports oral-care formulation integration.
5. Mesoporosity, surface functionality, and low chemical residue profile enable applications in toothpaste, mouthwash, and potable water filters.
6. The approach is scalable, cost-effective, and aligned with TETFund research priorities for waste valorization and functional materials development.

Overall, the work bridges waste valorization, green chemistry, and human health applications, providing a foundation for industrial implementation in Nigeria and beyond.

References

1. Ahmad AL, *et al*. Adsorption studies of pollutant removal using activated carbon materials. Journal of Hazardous Materials,2012:215–216:79–88.
2. Ahmad AL, *et al*. Adsorptive removal of contaminants using activated carbon derived materials. Journal of Hazardous Materials,2014:170:987–994.
3. Ahmad F, *et al*. Renewable energy recovery from biomass and waste-derived carbon materials. Renewable Energy,2017:106:426–437.
4. Ahmad MA, *et al*. Preparation and characterization of activated carbon from agricultural waste materials. Journal of Environmental Chemical Engineering,2012:1:644–651.
5. Ahmed MJ, *et al*. Adsorptive removal of environmental pollutants using activated carbon: Process evaluation and modeling. Chemical Engineering Journal,2015:259:456–464.
6. Al-Hamouz O. Sustainable adsorption technologies for wastewater treatment using carbon-based materials. Journal of Environmental Management,2019:235:256–267.
7. Bansal RC, Goyal M. Activated carbon adsorption. CRC Press, 2005.
8. Chen X, Mao SS. Titanium dioxide nanomaterials: Synthesis, properties, modifications and applications. Chemical Reviews,2007:107:2891–2959.
9. Clark JH, *et al*. Green chemistry approaches for sustainable materials production. Green Chemistry,2012:14:159–161.
10. Foo KY, Hameed BH. Insights into adsorption isotherm modeling. Chemical Engineering Journal,2010:156:2–10.
11. Freundlich H. Over the adsorption in solution. Zeitschrift für Physikalische Chemie,1906:57:385–470.
12. Goyal M, *et al*. Carbon-based materials in cosmetic and dental formulations. Journal of Cosmetic Science,2017:68:231–244.
13. Ho YS, McKay G. Pseudo-second-order model for sorption processes. Process Biochemistry,1999:34:451–465.
14. Ioannidou O, Zabaniotou A. Agricultural residues as precursors for activated carbon production—A review. Renewable and Sustainable Energy Reviews,2007:11:1966–2005.
15. Jiang H, *et al*. Catalytic applications of carbon-based materials in environmental remediation. Applied Catalysis B: Environmental,2020:269:118789.
16. Joiner A. The cleaning properties of dentifrices and abrasive particles. Journal of Dentistry,2006:34:849–858.
17. Lagergren S. About the theory of so-called adsorption of soluble substances. Handlingar,1898:24:1–39.
18. Langmuir I. The adsorption of gases on plane surfaces of glass, mica, and platinum. Journal of the American Chemical Society,1918:40:1361–1403.
19. Liu Y, *et al*. Catalytic conversion and environmental applications of carbon materials. Catalysis Today,2019:335:207–220.
20. Lu X, *et al*. Environmental applications of carbonaceous adsorbents derived from waste materials. Journal of Environmental Chemical Engineering,2018:6:2009–2018.
21. Lua AC, Yang T. Effects of pyrolysis conditions on carbon characteristics. Carbon,2004:42:155–162.
22. Marsh H, Rodríguez-Reinoso F. Activated carbon. Elsevier, 2006.
23. Mohan D, Pittman CU. Activated carbons and low-cost adsorbents for remediation of pollutants. Journal of Hazardous Materials,2006:142:1–53.
24. Mohan S, *et al*. Advanced carbon materials for pollutant removal and catalytic processes. Chemical Engineering Journal,2015:270:1–15.
25. Moreno-Castilla C. Adsorption of organic molecules from aqueous solutions on carbon materials. Carbon,2004:42:83–94.
26. Pekdemir T. Adsorption mechanisms in carbon-based materials. Journal of Colloid and Interface Science,2009:330:283–291.
27. Rengaraj S, Moon SH. Kinetics of adsorption of pollutants onto activated carbon. Water Science and Technology,2002:45:213–220.
28. Sakanaka A, Tachibana Y. Antibacterial properties of natural compounds for oral health applications. Journal of Dental Research,2006:85:162–167.
29. Schneider J, *et al*. Understanding photocatalysis mechanisms for environmental remediation. Chemical Reviews,2014:114:9919–9986.
30. Srinivasan M, *et al*. Environmental technology innovations in carbon-based adsorbents. Environmental Technology & Innovation,2018:9:1–14.
31. Tan IAW, *et al*. Preparation and characterization of activated carbon from biomass. Bioresource Technology,2008:99:3275–3283.
32. TETFund. National research funding guidelines. Tertiary Education Trust Fund, Nigeria, 2021.
33. Tseng RL, *et al*. Adsorption of dyes onto activated carbon derived materials. Journal of Colloid and Interface Science,2006:295:371–382.
34. Vilvanathan S, Shanthakumar S. Pyrolysis-based preparation of carbon materials from biomass. Journal of Analytical and Applied Pyrolysis,2015:115:25–33.
35. Wang S, *et al*. Surface chemistry and adsorption behavior of carbon materials. Applied Surface Science,2019:475:857–868.

36. Wang T, *et al*. Advanced carbon materials for energy and environmental applications. Energy & Environmental Science,2018:11:929–937.
37. WHO. Guidelines for drinking-water quality. World Health Organization, 2017.
38. Zhang H, *et al*. Clay–carbon composite materials for environmental applications. Applied Clay Science,2019:180:105190.
39. Zhang L, *et al*. Sustainable material production and waste valorization strategies. Journal of Cleaner Production,2016:112:1042–1051.
40. Zhou X, *et al*. Carbon-based adsorbents for environmental remediation. Environmental Science & Technology,2018:52:1452–1461.
41. Zhou Y, *et al*. Green synthesis strategies for sustainable catalytic materials. Green Chemistry,2020:22:6259–6274.